Solid State Communications, Vol. 30, 173–176.
Pergamon Press Ltd. 1979. Printed in Great Britain.

SOFT X-RAY EMISSION SPECTRA OF Zr IN Zr–H ALLOYS

K. Tanaka, N. Hamasaka and M. Yasuda

Department of Metallurgical Engineering, Nagoya Institute of Technology, Showa-ku, Nagoya 466, Japan

and

Y. Fukai

Department of Physics, Chuo University, Kasuga, Bunkyo-ku, Tokyo 112, Japan

(*Received* 25 *December* 1978 *by Y. Toyozawa*)

Zr–L_3 emission bands of ZrH_x alloys ($x = 0, 0.54, 0.95$ and 1.90) have been measured. With increasing x, a low-energy subband emerges and develops at 7 eV below the Fermi level at the expense of the intensity of the main band just below the Fermi edge. These changes in intensity cancel with each other, suggesting strongly that a remarkable redistribution of energy of $4d$ electrons at Zr sites takes place by the influence of protons on interstitial sites.

THE USEFULNESS of soft X-ray spectroscopy (SXS) for studying the electronic structure of metal–hydrogen alloys has been recently demonstrated in $VH(D)_x$ [1] and NbH_x [2]. The measurement of V–L_3 emission spectra of $VH(D)_x$ has given evidence of a gradual change of host d-band with the addition of H (D) and a formation of H (D)-induced states at the bottom of the d-band, in general agreement with results of theoretical energy-band calculations by Switendick [3]. Similar results have also been obtained in Nb–L_3 emissions of NbH_x. In contrast to these Va elements, where the hydrogen content is limited to x less than 0.8 under 1 atm of H_2 at room temperature, IVa elements (Ti, Zr and Hf) are known to accommodate hydrogen up to $x \sim 2.0$, and constitute another metallic group suitable for investigating the electronic structure of metal–hydrogen systems in a wider range of the hydrogen concentration. The present paper reports on measurements of Zr–L_3 emissions ($5s4d$-band $\rightarrow 2p_{3/2}$ level transition) in Zr–H alloys.

A reactor-grade Zr sponge (0.080 wt.% O and 0.078 wt.% Fe; purity > 99.8 wt.%) was loaded with hydrogen by holding at 600°C for 6 hr under purified H_2-gas flow, and slowly cooled. Next, the sample was successively dehydrogenated by annealing at 340 ~ 600°C for several minutes in vacuum, followed by slow cooling with valves of the vacuum furnace shut down. It was finally completely outgassed at 800°C in vacuum of 1×10^{-4} Pa. This procedure enabled us to prepare three ZrH_x alloys with $x = 1.90 \pm 0.10, 0.95 \pm 0.12$ and 0.54 ± 0.10, in addition to a pure Zr sample. The concentration was determined by gas-extraction analysis. The equilibrium phase diagram of the Zr–H system given by Beck [4] indicates the presence of ϵ-hydride (f.c.t.) for $1.66 \leqq x \leqq 2.0$; δ-hydride (f.c.c.) for $1.59 \leqq x < 1.66$; and α-phase (h.c.p. Zr) + δ hydride for lower x, at room temperature. The presence of γ hydride (ZrH) has also been suggested as a metastable product in the $\alpha + \delta$ region. The ϵ hydride is considered to have a fluorite structure with one cube axis contracted to a degree which depends on x. Based on this diagram, our samples are expected to be composed of following phases: $ZrH_{1.90}(\epsilon)$; $ZrH_{0.95}(\alpha + \delta)$; $ZrH_{0.54}(\alpha + \delta)$; and $Zr(\alpha)$. By X-ray diffraction analysis these phases were clearly identified in the samples, except for $ZrH_{0.95}$ and $ZrH_{0.54}$ where diffraction lines of only δ-phase were able to be detected. Since the measurement has been carried out not on powdered samples but on bulk crystals used for the SXS measurements, the diffraction lines of coexisting α-phase might have unexpectedly been missed in the latter samples.

The SXS measurements have been carried out in the same way as described in our previous report [1]. A curved ADP(110) crystal ($2d = 1.064$ nm; $R = 200$ mm) was used as an analyzer. The instrumental resolution at the Zr–L_3 band ($\lambda = 0.559$ nm) is rather poor and is estimated at 1.0 eV from a measured P–$K\alpha_1$ ($\lambda = 0.616$ nm) line width. The total resolution including the natural width of the Zr $2p_{3/2}$ level (~ 1.5 eV) [5] is estimated to be no less than 2.5 eV.

Figure 1 represents $L\beta_{2,15}$ (L_3 band) and $L\beta_3$ ($3p_{3/2} \rightarrow 2s$) spectra in pure Zr before hydrogen charging as a function of the photon energy. The L_3 band is located on the high-energy tail (dashed curve) of the $L\beta_3$ characteristic line, which is utilized as a standard of both energy and intensity of the L_3 band. The FWHM value of this band (4.4 ± 0.1 eV) is about 1 eV larger

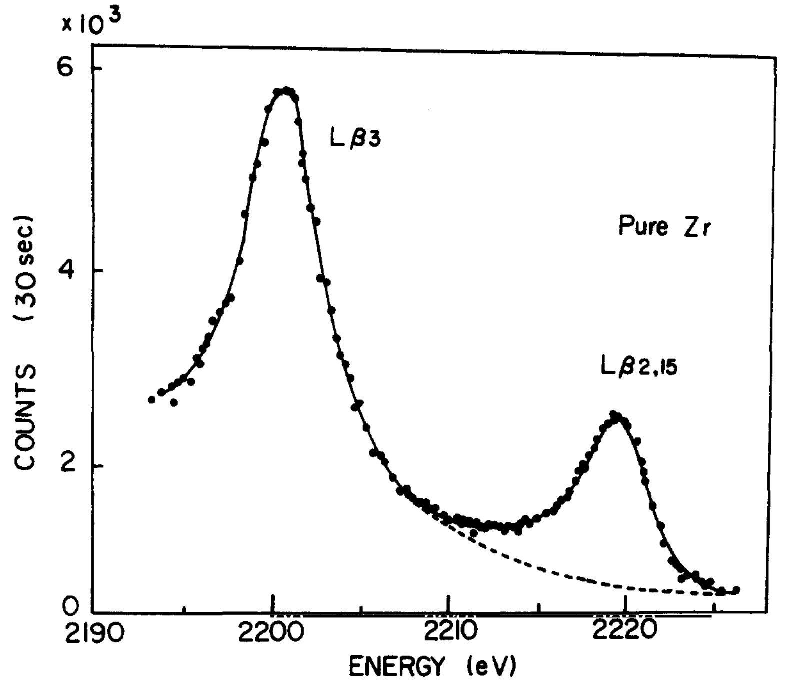

Fig. 1. $L\beta_{2,15}$ (L_3 band; *sd* band → $2p_{3/2}$) and $L\beta_3$ ($3p_{3/2}$ → $2s$) spectra in pure Zr.

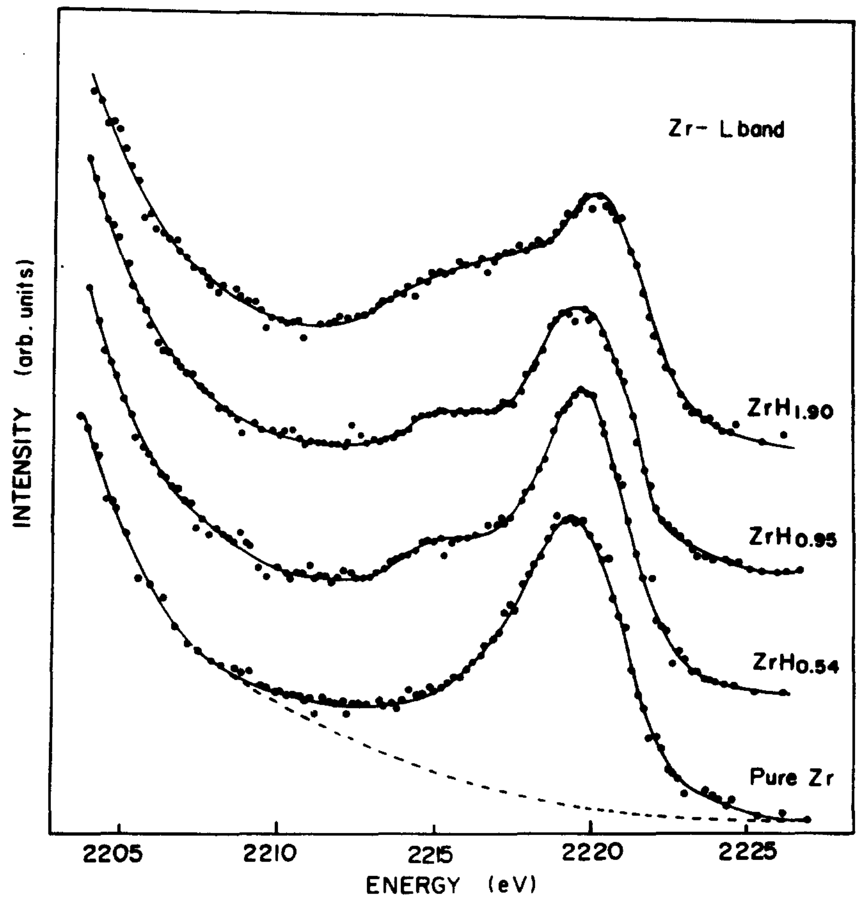

Fig. 2. Zr–L_3 band spectra in pure Zr and ZrH_x. The intensity of each spectrum is normalized to its $L\beta_3$ peak height.

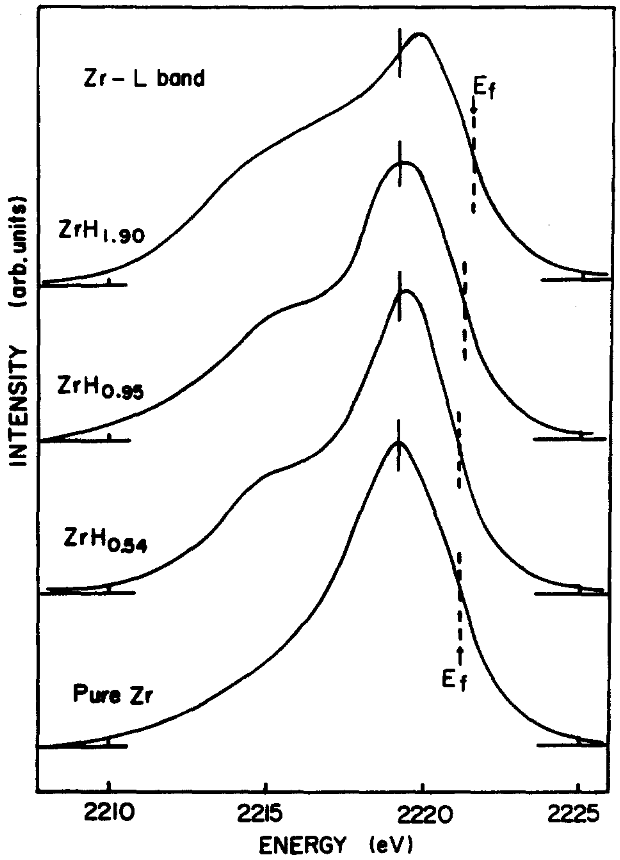

Fig. 3. Zr–L_3 emission bands after the $L\beta_3$ components have been subtracted.

Table 1. Increments in area of emission bands of ZrH_x *corresponding to* A, B *and* C *shown in Fig.* 4. *The whole area of the emission band of pure* Zr *is set to* 100

	Increments in area			
Samples	A	B	C	Total
$ZrH_{1.90}$	9.8	− 10.0	5.0	4.8
$ZrH_{0.95}$	6.4	− 6.4	1.8	1.8
$ZrH_{0.54}$	4.1	− 4.8	1.0	0.3

than a reported value [5], reflecting the difference of the instrumental resolution. Spectra of the L_3 band observed in ZrH_x are shown in Fig. 2 and are reproduced in Fig. 3 after the background contributions have been subtracted. The intensity of each spectrum in Fig. 2 is normalized to its $L\beta_3$ peak height. It must be mentioned here that a gradual alteration of spectral shapes due to escape of hydrogen from samples during measurements as observed in NbH_x [2] has never occurred in ZrH_x, and their SXS spectra have been found to be quite reproducible. We note the following features of the L_3 band of Zr–H alloys.

(1) A low-energy subband emerges and develops at 7 eV below the Fermi edge E_f (chosen at the half-height position) with the addition of hydrogen.

(2) The main band is depressed in height, and the Fermi edge is shifted toward higher energy as much as 0.5 eV in $ZrH_{1.90}$. It has been confirmed that these spectral changes due to hydrogenation are entirely restored when the samples are completely outgassed.

It may be helpful to make a comparison of the Zr–L_3 band of $ZrH_{1.90}$ with that of pure Zr, as shown in Fig. 4. Three features are evidently seen in the figure: an increment of the intensity at the low-energy subband

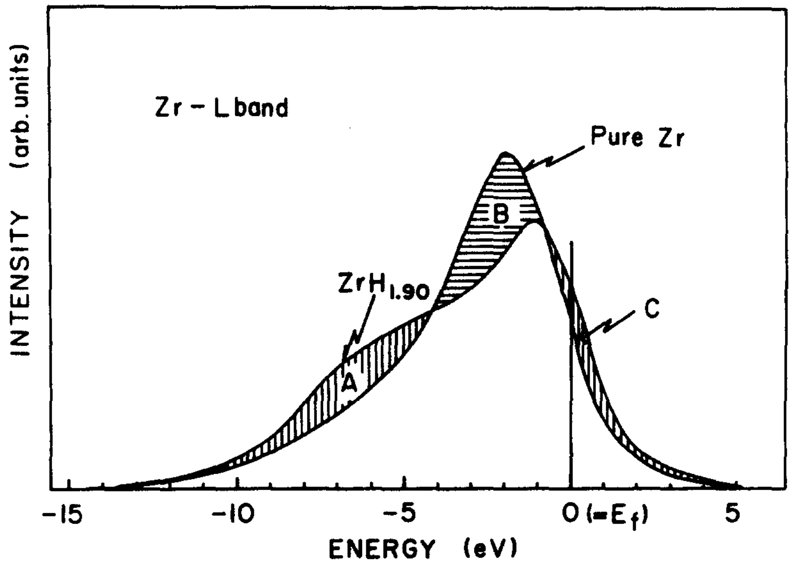

Fig. 4. Comparison of the Zr–L_3 band of $ZrH_{1.90}$ with that of pure Zr.

(A), a decrement at the main peak (B), and a small increment at the high-energy edge (C). Setting the whole area of the emission band of pure Zr to 100, changes in area corresponding to the regions A, B and C are tabulated in Table 1, including results on other samples. We find that in each alloy A and B cancel with each other within an experimental uncertainty, while C tends to increase slightly with increasing hydrogen content.

The low-energy subband found in ZrH_x corresponds evidently to those observed in V–L_3 and Nb–L_3 emission spectra in $VH(D)_x$ [1] and NbH_x [2], respectively. In addition, our recent study on the Ti–L_3 band in TiH_x [6] shows that it has spectral features which closely resemble those found in ZrH_x. These findings strongly suggest that the subband is due to a formation of bonding states between H–1*s* and metal–*d* states, which causes a heavy distortion of the host *d*-band structure of the metal. The fact that the decrement of the main band of the Zr–L_3 emission in ZrH_x is nearly complemented by the increment of its low-energy subband implies that the number of 4*d* electrons at a Zr site remains unchanged in spite of a significant redistribution of their energy through an interaction with surrounding interstitial protons. The slight increments of the area C on hydrogen loading could be associated with additional electrons supplied by hydrogen atoms filling up 4*d*-band holes. According to an energy-band calculation on TiH_2 (normal fluorite structure) [3], only 0.85 out of 2 electrons donated by hydrogen atoms are accommodated to fill up 3*d*-band holes of Ti, while the remaining electrons are supplied to an *sp* band pulled down below the Fermi level. This *sp* band is believed to be responsible for a distortion of the Ti–$K\beta_5$ emission observed in $TiH_{1.83}$ [7], but does not practically influence the L_3 emission band. Though detailed band-structure calculations on Zr–H alloys are not yet available, a rough estimation of the number of additional electrons in the 4*d*-band may be made from our present data. On the assumption that 4 valence electrons per Zr atom are contributing to the integrated intensity of the L_3 band of pure Zr, the number of the extra electrons in $ZrH_{1.90}$, given by the area C in Fig. 4, is estimated as $4 \times 5/100 = 0.2$. However, this would probably be an underestimate of its true value because of an appreciable self-absorption correction yet to be applied at the emission edge. To make a more quantitative analysis of the spectra, further corrections of the transition probability, Auger broadening and spectral resolution must be applied. Nature of *sp* band in ZrH_x may be understood by measuring Zr–M_5 emissions (5*p* band → $3d_{5/2}$). The measurement is now under way.

Acknowledgement – This work has partly been supported by the Grant-in-Aid for Scientific Research from the Ministry of Education.

REFERENCES

1. Y. Fukai, S. Kazama, K. Tanaka & M. Matsumoto, *Solid State Commun.* 19, 507 (1976).
2. E. Gilberg, *Phys. Status Solidi* (*b*) 69, 477 (1975).
3. A.C. Switendick, *Hydrogen in Metals I* (Edited by G. Alefeld & J. Völkl), p. 101. Springer-Verlag, Berlin (1978).
4. R.L. Beck, *Trans. ASM* 55, 542 (1962).
5. V.V. Nemoshkalenko, A.P. Shpak & V.P. Krivitskiy, *Fiz. Metal. Metalloved.* 39, 278 (1975).
6. K. Tanaka, N. Hamasaka, M. Yasuda & Y. Fukai (to be published).
7. S.A. Nemnonov & K.M. Kolobova, *Fiz. Metal. Metalloved.* 22, 680 (1966).